User-Centric Indoor Air-Quality Monitoring on Mobile Devices

Yifei Jiang, Kun Li, Ricardo Piedrahita, Yun Xiang, Lei Tian, Omkar Mansata, Qin Lv, Robert P. Dick, Michael Hannigan, Li Shang

■ *Because people spend a majority of their time indoors, indoor air quality (IAQ) can have a significant impact on human health, safety, productivity, and comfort. Because of the diversity and dynamics of people's indoor activities, it is important to monitor IAQ for each individual. Most existing air-quality sensing systems are stationary or focus on outdoor air quality. In contrast, we propose MAQS, a user-centered mobile sensing system for IAQ monitoring. MAQS users carry portable, indoor location tracking and IAQ sensing devices that provide personalized IAQ information in real time. To improve accuracy and energy efficiency, MAQS incorporates three novel techniques: (1) an accurate temporal n-gram augmented Bayesian room localization method that requires few Wi-Fi fingerprints; (2) an air-exchange-rate- based IAQ sensing method, which measures general IAQ using only CO_2 sensors; and (3) a zone-based proximity detection method for collaborative sensing, which saves energy and enables data sharing among users. MAQS has been deployed and evaluated through a real-world user study. This evaluation demonstrates that MAQS supports accurate personalized IAQ monitoring and quantitative analysis with high energy efficiency. We also found that study participants frequently experienced poor IAQ*

In recent years, indoor air quality (IAQ) has drawn considerable attention in both the public and scientific domains. This is mainly due to two reasons. First, people spend a majority of their time indoors, for example, about 90 percent for people in the United States. Second, most buildings appear to fall far short of reasonable air-quality goals (Huizenga et al. 2006). Statistics from the U.S. Environmental Protection Agency (EPA) indicate that, on average, the indoor levels of pollutants are two to five times higher than outdoor levels (U.S. Environmental Protection Agency Green Building Workgroup 2009). Bad indoor air quality influences human health, safety, productivity, and comfort (Wyon 2004; Daisey, Angell, and Apte 2003). Personal exposure to air pollutants is highly variable due to the presence of indoor air-pollution sources. Providing personalized IAQ information has the potential to increase public awareness of the relationship between people's behavior and air quality; help people to improve their living environments; and also provide valuable information to building managers, policy makers, health professionals, and scientific researchers.

IAQ monitoring is challenging because indoor air-pollutant concentrations and human motion patterns each vary spatially and temporally within and across rooms. These variations are caused by differences in user activities, number of occupants, and ventilation settings. For example, two office rooms in the same building may have sig-

 ISSN 0738-4602

nificantly different IAQ because of variation in the number of occupants (Huizenga et al. 2006). Existing solutions that require stationary sensors or target mobile outdoor sensing scenarios are inappropriate for personalized IAQ monitoring. Stationary sensing (Godwin and Batterman 2007) has several limitations. First, it can only measure the IAQ experienced by those who happen to be near the sensors and there can be substantial variation in IAQ even within one room. Second, when locations or rooms outnumber people, achieving full occupant coverage with stationary sensors is more expensive than doing so with personal mobile sensors.

A mobile sensing system designed for personalized IAQ monitoring must meet the following three requirements. First, the system requires accurate and reliable indoor localization techniques to detect user locations. Outdoor mobile sensing solutions use GPS localization, which fails indoors. Some existing approaches use proprietary radio frequency and ultrasound technologies for room localization, which require investment in infrastructure and special hardware worn by all users. Others use Wi-Fi-based fingerprinting, which requires time- consuming precharacterization and is hampered by device or environment heterogeneity. Second, the mobile sensing devices must be inexpensive and portable. This limits the number and types of sensors that can be integrated within each mobile device. Existing air-quality sensing solutions require multiple types of sensors, each of which covers a subset of pollutants. This can be prohibitively expensive for personalized mobile IAQ sensing. Achieving high-quality IAQ monitoring with inexpensive sensors is challenging. Third, the system needs to achieve a good balance between energy consumption and coverage. IAQ sensing depends largely on the motion patterns of individual users. This leads to redundant IAQ information when users are near each other and may lead to gaps in coverage for users who are not presently carrying sensing devices.

This article describes *MAQS*,[1] a personalized mobile sensing system for IAQ monitoring. MAQS estimates anthropogenic air-quality factors (for example, CO_2 and contagious viruses) using CO_2 concentration and estimates other air-quality factors (for example, volatile organic compounds [VOCs]) using air exchange rates. MAQS integrates smartphones and portable sensing devices to deliver personalized, energy-efficient, IAQ information. MAQS is the first mobile air-quality sensing system that achieves high coverage of people in indoor environments. Our work makes several main technical contributions: a temporal *n*-gram augmented Bayesian room localization method that is accurate and requires few Wi-Fi fingerprints; an air-exchange-rate-based IAQ sensing method, which measures general IAQ without requiring sensors for various types of air pollutants; and a zone-based proximity detection method for collaborative sensing, which saves energy and enables data sharing among multiple users.

The design of these three components demonstrates how artificial intelligence can be applied to enable innovative mobile phone applications. MAQS is a context-aware, energy efficient, and accurate IAQ monitoring system. Our room localization algorithm is able to determine the rooms occupied by users and associate them with measured indoor air-quality data. Our CO_2-based IAQ sensing method uses air exchange rate estimation and zone-based proximity detection to reduce energy use and increase IAQ estimation accuracy.

MAQS was evaluated through real-world system deployment and a user study. Our results demonstrate high accuracy (more than 96 percent for room localization and 89 percent for zone detection) and 2 times to 8 times better energy efficiency. Our IAQ analysis also reveals that most users in the limited study are subject to poor IAQ (that is, high CO_2 concentration and low air exchange rate) in a number of rooms.

System Overview

This section gives a high-level overview of the MAQS system architecture and describes its key components. As illustrated in figure 1, MAQS consists of four components: (1) M-pods, the portable IAQ sensing devices; (2) smartphones; (3) a data server; and (4) a web server. MAQS users carry smartphones and optionally M-pods. The data server communicates with clients, estimating and reporting room air quality, CO_2 concentration, and personalized IAQ data. The web sever allows users to view, analyze, and share IAQ data.

A MAQS client runs on each smartphone. It monitors the phone's accelerometer readings to detect room entering and departure events. For the purpose of IAQ monitoring, rooms are defined as enclosed building units with walls, doors, and windows where people spend substantial time (for example, office, classroom, or bedroom). We ignore transitional spaces indoors (for example, hallways). Once a client determines that its user has entered a room, the room localization function collects Wi-Fi signals from nearby access points and uses the subsequences of Wi-Fi signals (spatial informa-

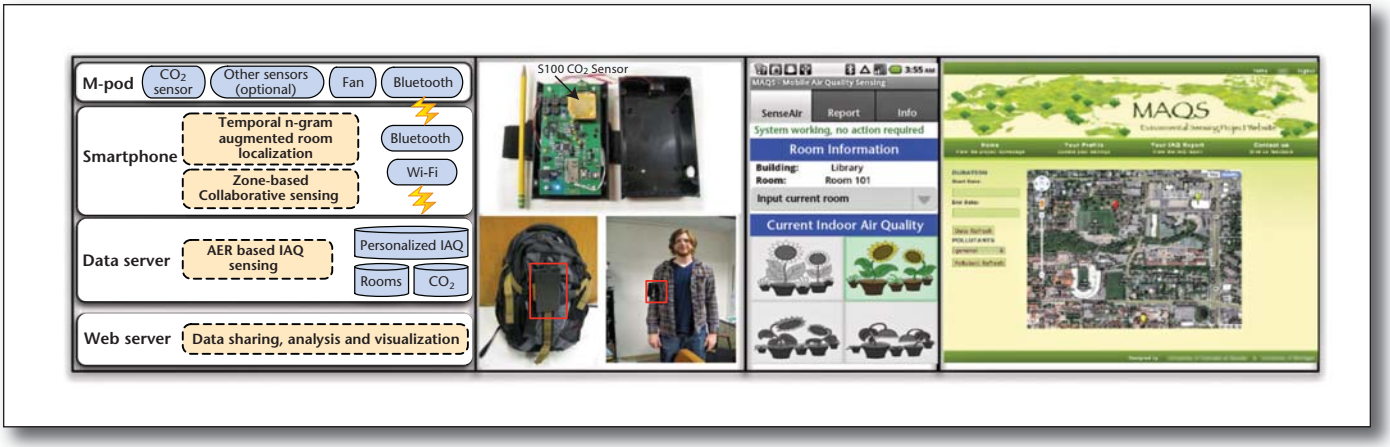

Figure 1. MAQS: User-Centered Indoor Air-Quality (IAQ) Monitoring on Mobile Devices.

tion) and the user's mobility pattern (temporal information) to determine the current room. The collaborative sensing unit then uses zone-based proximity detection to select a subset of sensing devices in the same room for (collaborative) IAQ monitoring of the room. This is useful since not all smartphone users carry IAQ sensing devices, and sensing devices close to each other (that is, in the same zone) are largely redundant. As CO_2, VOCs, and other air-pollutant[2] concentrations are collected and transmitted to the server, they are stored in databases and combined with room information (for example, room ID and volume) for air exchange rate estimation and personalized IAQ analysis. MAQS stops IAQ sensing after detecting room departure and restarts when another room is entered.

M-pod: The Portable IAQ Sensing Device

Our system design requires a mobile IAQ sensing device with multiple accurate, low-cost sensors. It must also connect wirelessly with smartphones and have a long battery lifespan. Existing designs did not meet these requirements, so we developed a new sensing device called the M-pod. The M-pod is a wireless embedded sensing, computation, and communication device based on the Arduino platform.[3] It can sense multiple air pollutants and either store the data locally or transmit them to nearby smartphones using Bluetooth.

M-pod Hardware Design

The M-pod's major components are an 8-bit, 32-pin microcontroller, a Bluetooth module, and up to 10 on-board sensors, all mounted on a custom-fabricated four-layer printed circuit board. Table 1 lists the processor, wireless interface, and sensors.

Hardware	MCU	Bluetooth	Battery	Size (inch)
specifications	ATMEGA 168	WT11	CS HDE160XL	4.8 x 2.6
On-board	Temperature	CO_2	Humidity	Light sensors
sensors	TMP101	S100	HYT271	GL5528

Table 1. M-Pod Processor, Wireless Interface, and Sensorsing on Mobile Devices.

The humidity sensor, two temperature sensors, and CO_2 sensor are connected to the microcontroller through the I2C interface. The other sensors are attached to the microcontroller's analog-to-digital converter interface. The metal oxide gas sensors are power gated using PMOSFETs when idle to maximize battery lifespan. A 5 V DC fan is mounted to the case. The sensors are positioned to enable uniform airflow. When sensing, the fan moves air at a rate of 2 liters per minute, thereby minimizing sensing latency when IAQ changes.

Energy Consumption

The M-pod is powered by a 2200 mAh Lithium-ion battery, which can be recharged using a standard wall-mounted AC–DC converter. The Lithium-ion battery is protected by an interlock that halts the system when the battery voltage drops below 2.9 V. The M-pod requires 240 milliwatts in low-power mode, in which only the processor and CO_2, humidity, and temperature sensors are enabled. It requires 1080 milliwatts when, in addition, four metal oxide gas sensors are activated. The fan requires up to 105 milliwatts, but this can be reduced through pulse-width modulation. The Bluetooth interface needs to transmit so infrequently in this application that its power consumption has little impact on battery lifespan. The battery lifespan is approximately 5.5 hours if an M-pod is continuously active and greater than 24 hours when in low-power mode.

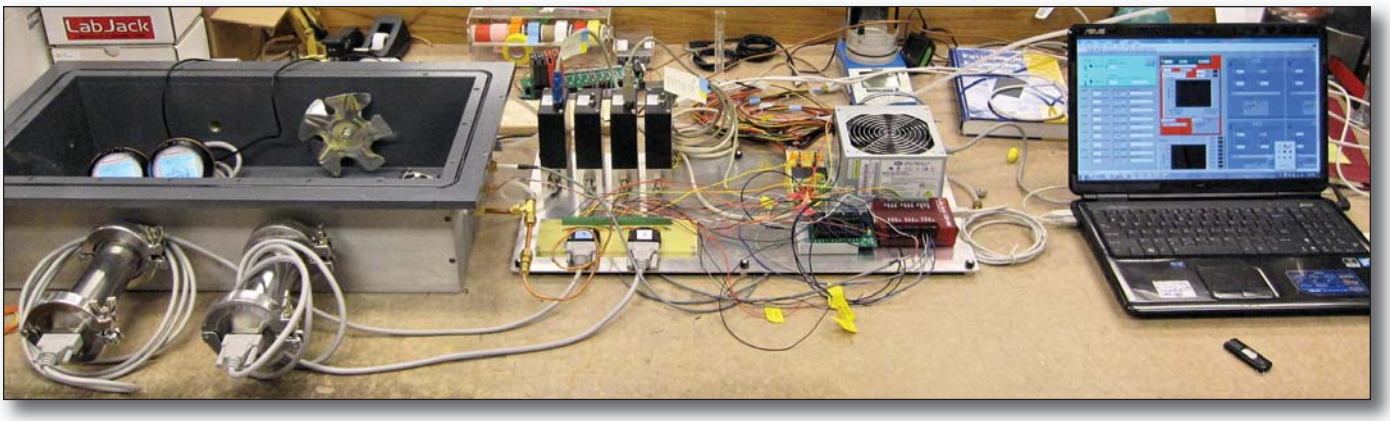

Figure 2. PC Interface and Data Acquisition System.

Left: The calibration chamber with the mass flow control. *Right:* The data acquisition system.

Command Processing

The M-pod processes low-power mode, full-sensing mode, power state inquiry, and transmit data commands, which are generally received from smartphones. IAQ sensor readings are collected every six seconds and stored in the microcontroller's SRAM. In low-power mode, the metal oxide sensors are power gated because they contain resistive heating elements with high power consumptions. The power state inquiry command transmits the current mode to the requester. The data transmit command uploads the data stored on the M-pod to the requester.

Latest Development

The latest version of the M-pod has been revised to triple the battery lifespan, halve the size, and improve reliability by using communication error recovery algorithms, among other improvements. The average power consumption, when power cycling is disabled, is reduced to about 160 milliwatts. Specifically, when communication is disabled and the sensing interval varies from 1 to 15 seconds, the power consumption of the M-pod ranges from 154 milliwatts to 159 milliwatts. Also, when the sensor sampling rate is fixed at 1 Hertz and the transmission interval varies from 1 to 15 seconds, the M-pod's power consumption ranges from 157 milliwatts to 168 milliwatts. On average, the new M-pod can work continuously for more than 15 hours.

CO_2 Sensor Calibration

Many low-cost air-quality sensors are challenging to work with. Their baseline readings can drift over time, response time can be slower than desired, and sensitivity to the target pollutants can change over time, or the sensors may be exposed to compounds that degrade them. Many also suffer from high cross-sensitivities, causing them to respond not only to the target gas but to other pollutants of less interest (including water vapor).

Nondispersive infrared (NDIR) CO_2 sensors suffer from few of these problems. Instead of relying on chemical reactions, NDIR sensors measure CO_2 concentrations by observing the absorption of infrared light by CO_2. They have good linearity, high repeatability, and low response time. Although H_2O is also absorbent in the infrared spectrum, our tests show that the NDIR sensors we used are mostly insensitive to humidity. They were thus the first sensors we used when developing and evaluating the MAQS system. The sensors were calibrated in a custom chamber multiple times throughout the experiment. To calibrate, the M-pods were placed within the teflon-coated chamber and precise gas mixtures were fed in through nonreactive tubing. Gas flows were administered using mass flow controllers (MFCs), which were controlled using a PC interface and data acquisition system, as shown in figure 2.

Figure 3 shows a typical calibration run, in which the sensors were exposed to three different pollutant concentrations. For CO_2, these concentrations are generally near 0 parts per million, 400 parts per million, and 1600 parts per million, with the balance gas being nitrogen. The calibration process is designed to be performed quickly (approximately 15 minutes at each concentration setting). The calibration fit in figure 4 shows the linear fit between sensor output signal and concentration. Uncertainty in the sensor signal is calculated from the calibration fit by estimating the standard deviation of regression, which is then propagated through the calibration function, providing uncertainty estimates for the ambient data. The signal uncertainty at each concentration in a typical calibration is shown in figure 4. The average measurement of uncertainty for these data was found to be 39.8 parts per million, with a standard deviation of 8.6 parts per million.

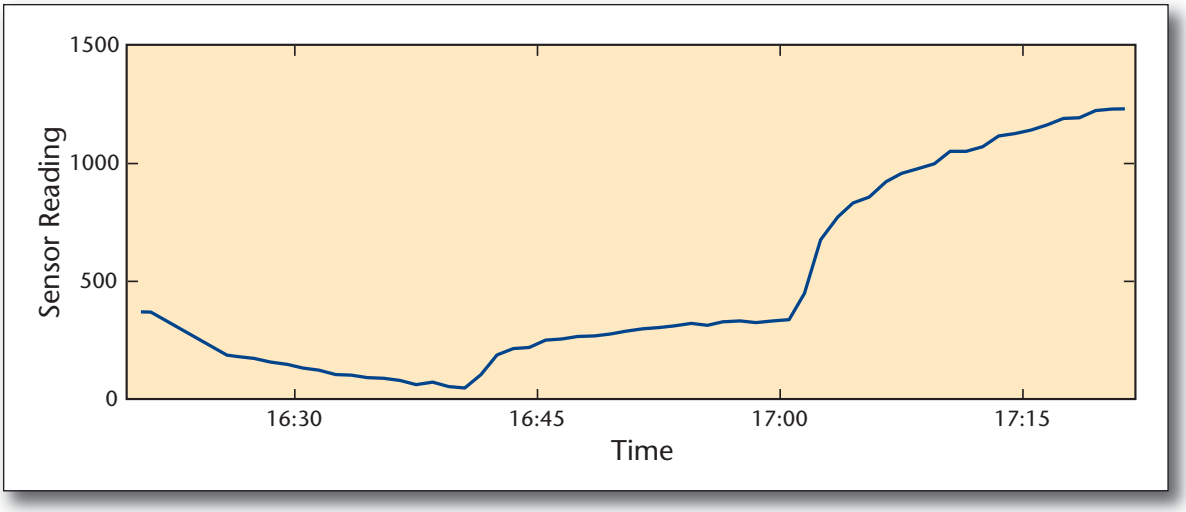

Figure 3. CO_2 Calibration Time Series Example Data,

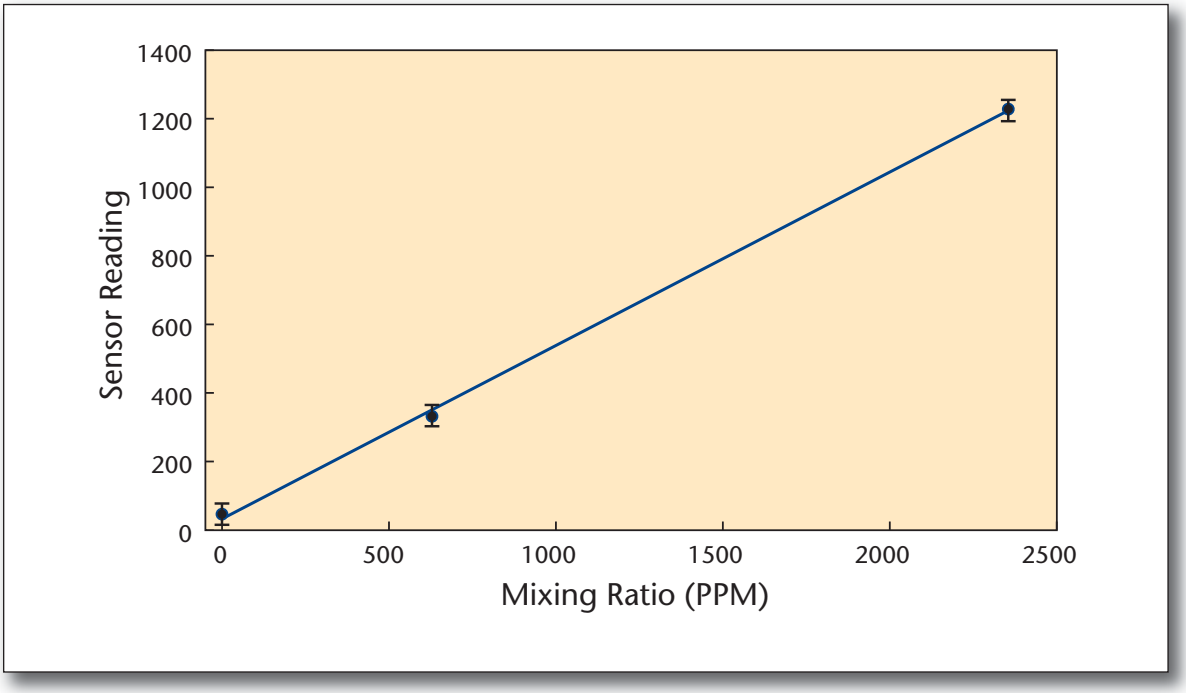

Figure 4. Example of a CO_2 Calibration Curve Fit.

The black dots represent the calibration points, while confidence intervals are shown by the accompanying bars.

Room Localization

M-pods are carried by users, that is, their locations change as users move. The collected IAQ data is valuable for data analysis, visualization, and sharing only when it can be associated with the appropriate source room. Room characteristics correlate closely with IAQ and rooms are the basic control units in building management. Hence accurate room localization is required for personalized mobile IAQ monitoring.

Researchers have proposed two-stage room localization techniques based on Wi-Fi access point received signal strength (RSS) (Park et al. 2010; Haeberlen et al. 2004). In the first (training) stage, a database that associates ambient Wi-Fi RSS fingerprints with physical rooms is constructed. In the second (operating) stage, the system identifies the stored Wi-Fi fingerprint most similar to current measurements, and returns the associated room.

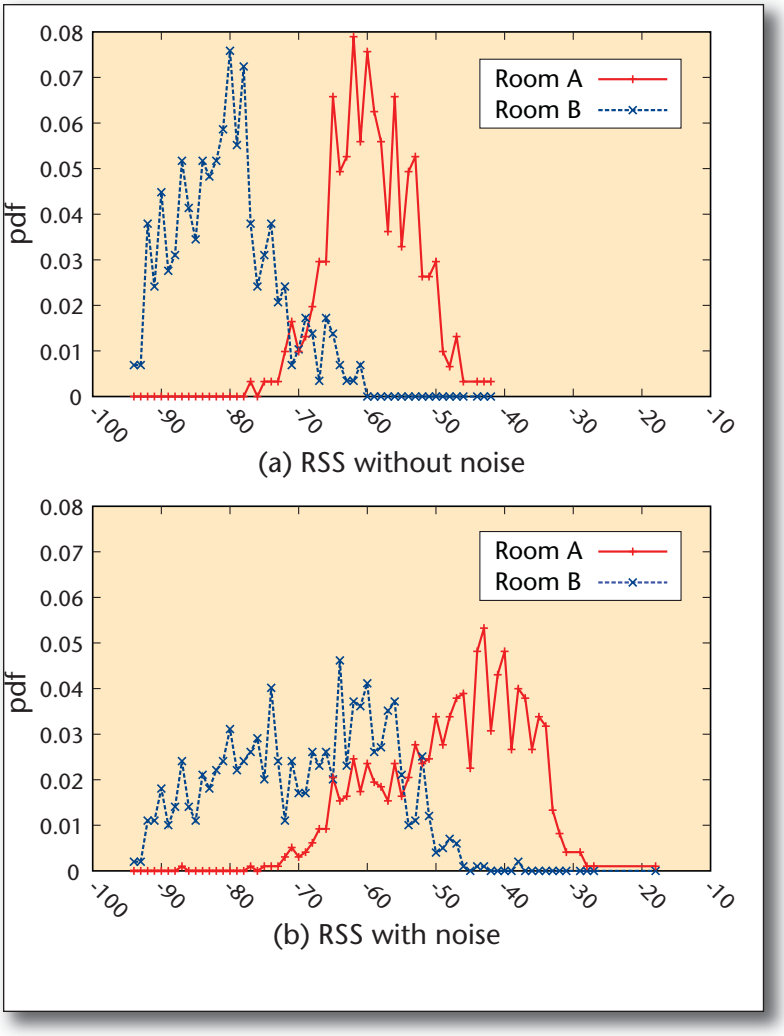

Figure 5. Wireless RSS Distributions in Two Adjacent Rooms.

(a) Without noise. (b) With environment and device noise.

The first stage of our room localization technique is similar to that of Park et al. (Park et al. 2010). All users contribute their Wi-Fi RSS and room information to create a shared database of room fingerprints. This is beneficial because it (1) eliminates the deployment cost for fingerprint presampling and (2) reduces user effort to build the database.

In the second stage, Bayesian room localization models are commonly used (Haeberlen et al. 2004; Park et al. 2010). Under these models, the learned database includes all fingerprinted rooms R, and the fingerprint of each room r ($r \in R$) is represented as a probability table for each access point (AP) with different RSS values that was observed in the room. Given a Wi-Fi measurement o, a Bayesian model is used to compute $P(o|r)P(r)$ for each room r in the database and the room with the highest probability is selected as the room that the user is most likely to be in. Let w_i be the RSS value of the ith AP in the Wi-Fi measurement o. Then the probability of observing o in room r, $P(o|r)$, can be computed as

$$\prod_i P(w_i \mid r)P(r)$$

Note that we can obtain $P(w_i|r)$ from the probability table in the database.

This model is based on the assumption that the AP signal strengths observed by the mobile device are conditionally independent. However, the model fails to address the following two challenges: (1) device heterogeneity — different devices may be used for gathering RSS fingerprints and devices might be held differently (for example, in hand, pocket, or bag) and (2) temporal variation — the wireless environment of a room may change over time, due to motion of people and other room contents, influencing the RSS fingerprints gathered by mobile devices. As demonstrated in figure 5, noise induced by device heterogeneity and temporal variation significantly increase the RSS overlap between adjacent rooms, reducing room localization accuracy. To address these problems, we first characterize Wi-Fi signal variations due to the above two factors and explain how they affect the room localization. These observations motivate the design of a novel temporal n-gram augmented Bayesian room localization method that is robust to both temporal and device noise.

Characterization of Wi-Fi Fingerprint Variation

Each Wi-Fi sample obtained by a mobile device consists of a list of APs and the received signal strength value from each AP. Depending on how Wi-Fi fingerprints are constructed, two different types of information may be used: occurrence (OCC) and received signal strength (RSS).

Occurrence (OCC) refers to whether a specific AP or a set of AP occurs in a Wi-Fi sample or not. Each mobile device scans all available APs a total of N times. If we assume k-combination APs ($k \geq 1$) occurred m times among the N samples, then the occurrence rate of k-combination APs is m/N. We also consider the occurrence rate of ordered k-combination APs. That is, given a Wi-Fi sample, we first order the set of APs by their corresponding RSS values, then generate k adjacent APs.

Received signal strength (RSS) is a commonly used feature in room localization. The RSS of each AP can be measured directly. Its value is relatively stable within a room, yet changes significantly when crossing walls. We characterize Wi-Fi signals for the RSS values of single APs and for differences between pairs of AP RSS values. Similar to OCC, we consider both k-combination of APs (that is, any two APs) and ordered k-combination of APs (that is, adjacent APs in the sorted sequence based on descending RSS values).

We conducted a set of controlled experiments to characterize variations of Wi-Fi fingerprints. Seven different phones (see table 2) were used to capture device heterogeneity. We collected Wi-Fi fingerprints for a set of adjacent rooms in different buildings, which are shown in table 3.

Device Heterogeneity

To characterize Wi-Fi fingerprints in the presence of device heterogeneity, we used seven different smartphones to collect Wi-Fi signals in two adjacent rooms and then compared both OccRate-Diff and RSS-Diff RSS distributions for each pair of different phones, such as HTC Sensation versus Samsung Galaxy S2. In each experiment, the seven phones were placed together at one position. We then moved the phones to a different position (in the same room or in the adjacent room) that was 2 meters away from the original position. Each experiment lasted 10 minutes. To minimize temporal variation, there were minimal delays between experiments. The experiments were done during the night, when the wireless environment was most likely to be stable.

Phone	Manufacturer	Release Date
HTC Sapphire	HTC	2009-02
HTC Hero	HTC	2009-07
DROID	Motorola	2009-10
N900	Nokia	2009-11
Nexus One	Google	2010-01
Galaxy S2	Samsung	2011-02
HTC Sensation	HTC	2011-04

Table 2. Phone Types Used for Data Collection

Building Type	Number of Rooms	Number of Experiments per Room
Educational	18 adjacent rooms on three floors	10 times in 1 month
Commercial	12 adjacent rooms on three floors	10 times in 1 month
Residential	8 adjacent rooms on three floors	10 times in 1 month

Table 3. Controlled Experiments

Figures 6a–e shows the cumulative distribution function (CDF) curves of occurrence rate difference (OccRate-Diff) for different device combinations, using different *k*-combinations of APs ($k = 1, 2, 3$) and ordered *k*-combinations of APs ($k = 2, 3$). The same-room and cross-room Wi-Fi curves can be separated, especially when $k = 1$ and 2 (see figure 6a–b). However, the distributions within the same room (the dark or light curves) are not well concentrated. This shows the variation among devices. As *k* increases (see figure 6c), the same-room distributions become more similar but there is also increased overlap between same-room distributions and cross-room distribution, that is, reduced separation power. In figure 6d–e, we can see that the distribution curves within a room are concentrated, which makes room recognition easier. However, most of the curves overlap cross-room curves. As a result, it is difficult to use the ordered *k*-combination of APs for room localization.

To understand how device heterogeneity affects RSS-based fingerprints for room localization, we draw the CDF of RSS difference (RSS-Diff) for each pair of devices, when using different *k*-combinations ($k = 1, 2$) and ordered 2-combinations. As shown in figure 6f–h, in all three plots, there are large differences among the same-room curves. In other words, when different devices are used, the RSS-based Wi-Fi fingerprints can vary significantly within the same room. Such poor concentration makes it difficult to identify a specific room using RSS-based fingerprints. However, there is good separation between the same-room and cross-room curves, especially with 2-combination APs and ordered 2-combination APs (see figure 6g–h). Also, ordered 2-combination APs slightly outperform unordered 2-combination APs because there is better concentration of same-room curves when for ordered 2-combinations, thus increasing the ability to identify specific rooms and distinguish different rooms.

Temporal Variation

To characterize Wi-Fi fingerprints under temporal variations, we used one phone to collect Wi-Fi signals in one room at different times during the morning, noon, afternoon, evening, and night and then collected Wi-Fi signals with the same phone on another two days in the same room and adjacent room at a position that is 2 meters from the first experiment position. We used the 2-meter distance for both same-room and cross-room experiments. In each experiment, we collected Wi-Fi signals over a time window of 10 minutes, obtaining one sample every 5 seconds. Then, to calculate OccRate-Diff and RSS-Diff for different (ordered) *k*-combinations, we consider Wi-Fi samples collected in pairs of time periods, such as morning versus afternoon or noon versus evening.

Figure 7a–e shows the CDF curves of OccRate-Diff for different time periods, using different *k*-combination of APs ($k = 1, 2, 3$) and ordered *k*-combination of APs ($k = 2, 3$) as the fingerprint. The red (blue) curves represent same-room (cross-room) scenarios during different time periods. First, we can observe that in all five plots, the same-room and cross-room curves overlap heavily and are therefore difficult to separate. Therefore, none of the occurrence-based Wi-Fi fingerprints are good at distinguishing rooms. Our results also confirmed the observation (Haeberlen et al. 2004) that real-time signal distributions often differ from those in the training phase. However, despite different tem-

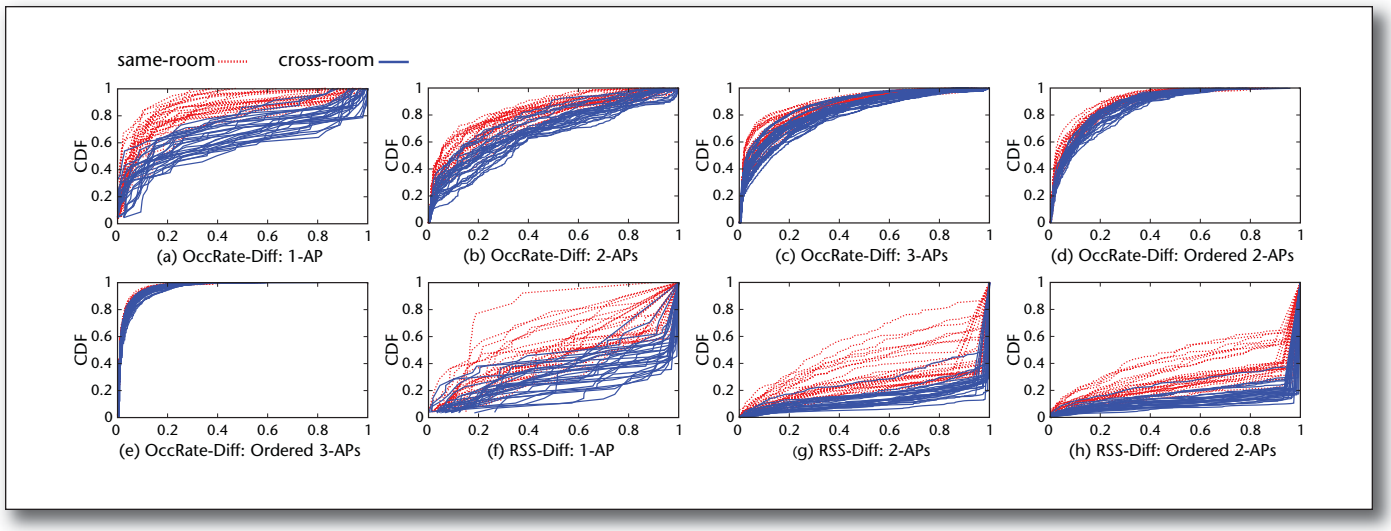

Figure 6. Device Variation.

CDF of OccRate-Diff(a, b, c, d, e) / RSS-Diff(f, g, h) using different occurrence-based Wi-Fi fingerprints.

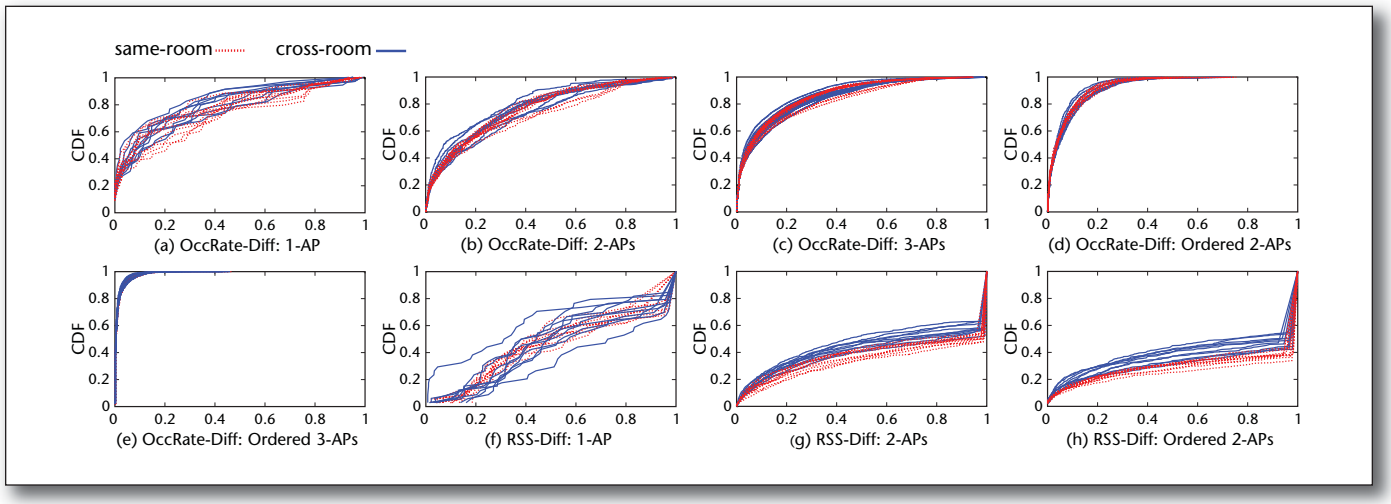

Figure 7. Temporal Variation.

CDF of OccRate-Diff(a, b, c, d, e) / RSS-Diff(f, g, h) using different occurrence-based Wi-Fi fingerprints.

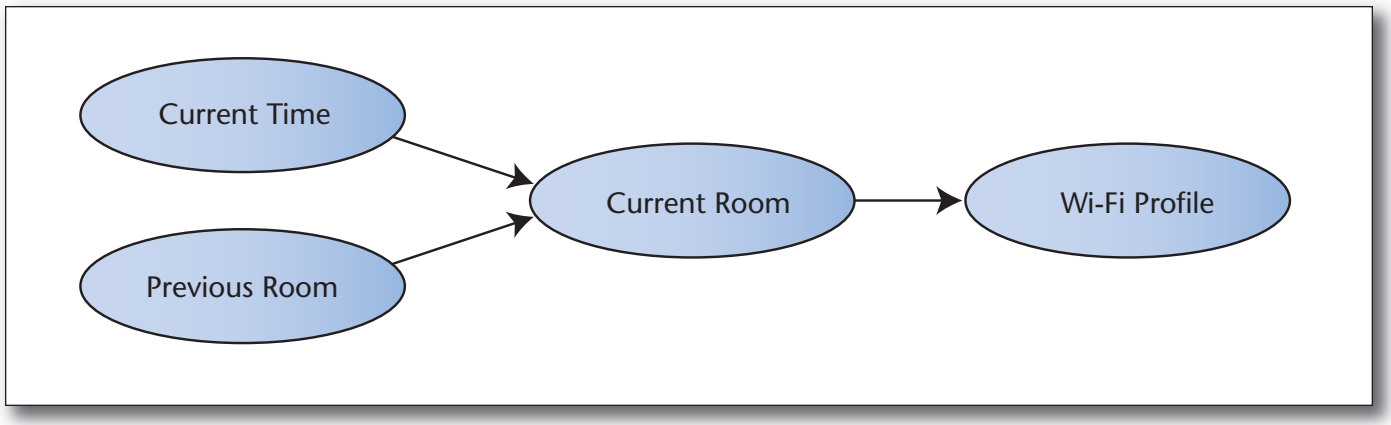

Figure 8. Bayesian Network for Room Localization.

poral variations, we do see good concentration of same-room curves, especially when ordered *k*-combination is used.

Figure 7f–h shows the CDF curves of RSS-Diff for different time periods, using 1-AP, 2-APs, and ordered 2-APs as fingerprints. Again, the light (dark) curves represent same-room (cross-room) scenarios during different time periods. From figure 7f, we see that same-room and cross-room curves heavily overlap, that is, there is low distinguishing power. There is also a large spread among same-room curves, indicating poor concentration. The good news is that both 2-APs and ordered 2-APs perform well despite temporal variation. As shown in figure 7g–h, the same-room and cross-room curves are well separated, indicating high differentiating power for room localization. Moreover, both types of fingerprints also have good concentration for same-room scenarios.

N-gram Augmented Bayesian Room Localization

Our key observation is that, although the exact RSS values of each AP may change substantially for different devices and environments, the *ordered sequence of APs based on their RSS values tends to be similar for the same room and inconsistent among adjacent rooms*. For example, the ordering may be $[ap_1, ap_2, ap_3, ap_4, ap_5, ap_6]$ at one time, and $[ap_2, ap_1, ap_3, ap_4, ap_5, ap_6]$ at another time, for the same room. The ordered AP sequences of adjacent rooms are less similar, especially when different APs are observed in these rooms. Intuitively, the ordered AP sequence is useful for room localization because (1) it captures the inherent correlations among APs, which are stable for the same room yet different for adjacent rooms and (2) it uses the order of RSS instead of their exact values, allowing many sources of device variation and wireless environment variation to be tolerated.

Based on the observations above, we propose an *n*-gram augmented Bayesian room localization model, which works as follows. For a given ordered AP sequence of Wi-Fi scan *s,* we consider for each room *r* the probabilities of seeing subsequences of *n* continuous APs in *s,* that is, *n*-grams. According to our experimental results, we set $n = 2$ in order to achieve the best accuracy for room localization. Our new model computes $P(RSS(2\text{-}gram(s))|r)P(r)$ using the Bayesian model for each room *r* in order to determine the room that the user is most likely to be in. The RSS of a 2-gram is defined as the absolute value of the difference between the RSS values of the two adjacent APs in the ordered sequence.

Temporal User Mobility for Room Localization

As shown in the experimental results, our *n*-gram augmented Bayesian room localization model achieves high accuracy when the room has enough fingerprints (more than 50 or 100). However, when the number of fingerprints is low, the model accuracy is poorer and users tend to be misclassified into nearby rooms. To remove such spatial errors, we propose to incorporate temporal user mobility information. This is motivated by the following observations:

> A user's current room is closely related to time and day of the week; for example, the user has weekly meetings in the conference room on Tuesday mornings.
>
> Users can only move among adjacent rooms, and their paths tend to contain patterns. For example, a user usually goes to the conference room from her office instead of from a classroom.

Therefore, a user's current room can be predicted based on the current time and her previous room location. As shown in figure 8, the Bayesian network has three layers: current time and user's previous room (first layer) indicate the user's current room (second layer), and the user's current room determines the observed Wi-Fi RSS fingerprint. We also define a set of values to represent some semantic concepts of time, including "day of week," "morning," "afternoon," and "evening." Given a Wi-Fi scan observation *s*, the user's previous room r', and current time *t,* the probability of the user staying at room *r* is $P(s, r, t, r')$. Based on the joint probability function, the probability value is equal to $P(s|r)P(r|t, r')P(t)P(r')$. $P(s|r)$ can be computed using our *n*-gram augmented Bayesian room localization model. $P(r')$ and $P(r|t, r')$ are calculated from the user's mobility history. $P(t)$ can be ignored since it is the same for any room *r.*

Air-Exchange-Rate-Based IAQ Sensing

Indoor air quality is influenced by multiple air pollutants and sources, including (1) air pollutants generated indoors, such as volatile organic compounds (VOCs), from combustion and off-gassing of paint and building materials; (2) air pollutants introduced from outside through ventilation, for example, ozone; and (3) air pollutants generated by people, for example, CO_2. It is impractical to install sensors on our portable IAQ sensing devices to monitor all pollutants of interest, as the sensing device would become unreasonably large and require too much power. Additionally, not all pollutant sensors are portable, and portable sensors are typically less accurate than stationary sensors. As shown in previous studies (Seppänen, Fisk, and Mendell 1999; Persily 1997; Daisey, Angell, and Apte 2003; Fisk, Mirer, and Mendell 2009), CO_2 concentration and ventilation rates are strongly correlated with general IAQ. Therefore, the M-pod

monitors CO_2 concentration, which is then used to estimate the air exchange rate, that is, how quickly air is cycled through a room. This rate is used to estimate general IAQ in a room. Specifically, personalized air exchange rates are modeled using changes in CO_2 concentration and CO_2 generation rate. The rate of change in CO_2 concentration depends on the concentration in in-flowing air, the concentration in out-flowing air, and the internal generation rate of CO_2 in a room. The air exchange rate equation is given by Persily (1997). That is calculated based on internal concentration of CO_2, external concentration of CO_2, generation rate of CO_2 in the room, and room volume.

In our system, internal concentration of CO_2 is collected from the M-pod. External concentration of CO_2 is set to 390 parts per million, the globally averaged CO_2 concentration at the surface,[5] unless local outdoor CO_2 concentration is available. To calculate the CO_2 generation rate, we assume each person's generation rate is equal to 0.0052 L/s (Persily 1997), which corresponds to an average-sized adult engaged in office work. At this time, we do not incorporate other possible sources of CO_2 such as cooking or smoking. Room volume V can be provided by the user through our system, or it can be calculated from CO_2 data based on the steady-state concentration balance equation, that change of CO_2 is equal to zero. The air exchange rate required for good IAQ depends on the size and occupancy of each room. In our system, three metrics are considered for IAQ, as follows:

Indoor CO_2 concentration is a surrogate for indoor pollutants emitted by humans and correlates with human metabolic activity. The ASHRAE Standard is at most 700 parts per million above outdoor CO_2 concentration.[4]

Air changes per hour is a measure of how many times the air within a defined space (normally a room or house) is replaced per hour. Its value equals the air exchange rate of room divided by room volume. The ASHRAE standard is at least 0.35 1/h (Sherman 2004).

Air flow per person is the room air exchange rate divided by the number of people in the room. The ASHRAE standard is at least 7.5 l/s/person (Sherman 2004).

Zone-Based Collaborative Sensing

In real-world usage scenarios, multiple users are likely to stay in the same room, for example, in meeting rooms or the library. Such user groups tend to be concentrated in small areas, leading to similar CO_2 concentration and IAQ within each group. Through collaborative sensing, we aim to reduce the number of sensing devices that must run concurrently (thus saving energy), and also enable IAQ data sharing with people who do not carry sensing devices (thus increasing system coverage and utility).

Many low-cost sensors used in mobile sensing devices are susceptible to drift error. Calibrating with an accurate stationary sensor can reduce this error. However, in real-world applications, the stationary sensors are usually scarce. Therefore, opportunities for accurate calibration are rare. The collaborative calibration technique (Xiang et al. 2012) supports calibration among inaccurate mobile sensing devices. It can significantly increase the calibration opportunities and thus improve the sensor accuracy. To implement this technique, sensors must be able to detect when they are within calibration range of each other.

We propose using a zone-based proximity detection and information sharing mechanism. Concentration gradients are driven by transport through molecular diffusion and convection. Both transport processes have random and nonrandom components. Whatever the process, the spatial gradients dictate that two nearby points will have more similar concentrations than two distant points. In MAQS, we define an area with high density of people as a *zone*. All people within the same zone can share one M-pod for IAQ monitoring. When a new user without an M-pod joins this zone, the user's smartphone initiates a scan to determine if there is already an M-pod in the zone. If so, a communication link between the phone and the M-pod is established and the IAQ values reported by the M-pod are used to estimate the IAQ of this user. If a new user joins the zone with her M-pod, after the collaborative calibration, only one M-pod in the zone will perform the sensing and the rest of the M-pods can be turned off to save energy.

Zone-based sharing would incur some error, which is defined as the difference between the CO_2 concentration reported by the shared M-pod nearby and the true CO_2 concentration at the user's location. According to the diffusion equation, this error is correlated with the separation distance. Therefore, this error determines the effective range of each zone.

We conducted more than 50 experiments to determine the relationship between distance and CO_2 error in public rooms, including classrooms and a library. In each experiment, two M-pods are placed 1–10 meters apart for more than 20 minutes. The CO_2 readings from both M-pods are monitored and the corresponding air exchange rates are calculated. Figure 9 shows the sensing error rate for CO_2 concentration at different separation distances. Ranges less than 2 meters enable better and more consistent results. Two meters is therefore used as the range threshold of zones in the MAQS system.

Given the zone range threshold (2 meters), each

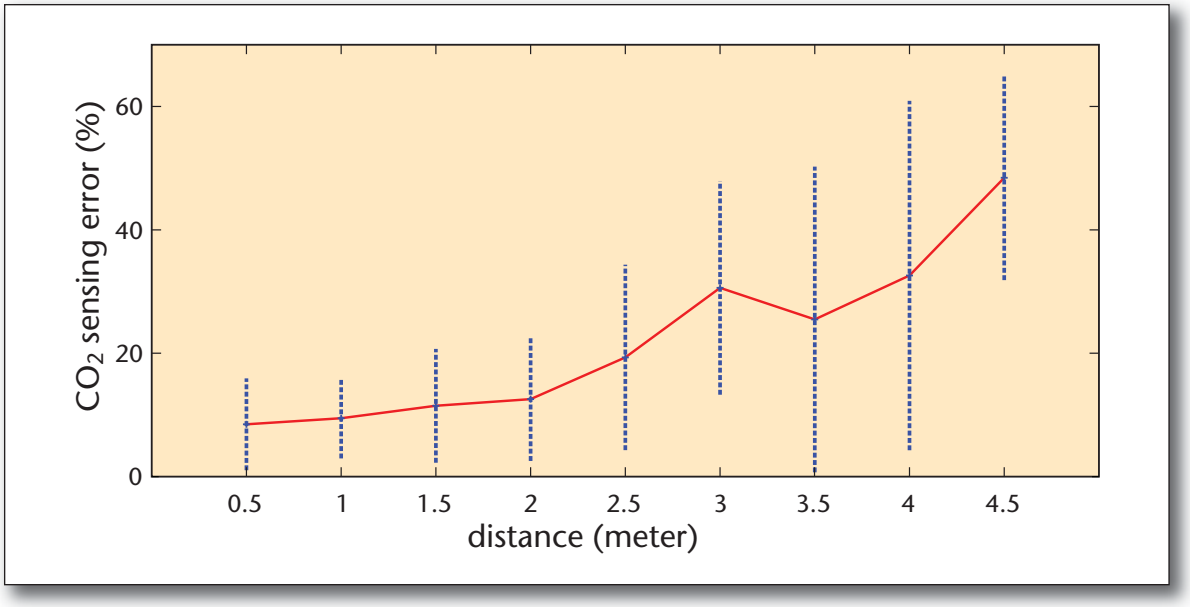

Figure 9. Sensing Error of CO_2 Concentration at Different Distances.

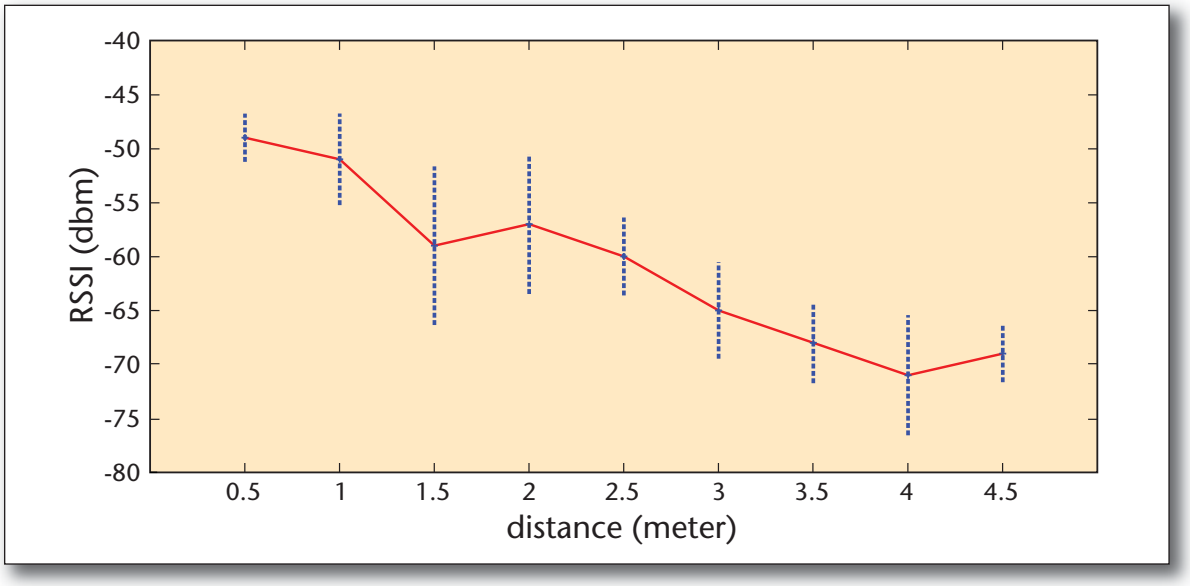

Figure 10. RSSI Measurements (Average and Standard Deviation) at Different Distances.

smartphone still needs to determine how far away a specific M-pod is. In MAQS, we use the received signal strength indication (RSSI) from the Bluetooth radio to estimate distance. The signal power of Bluetooth communication can be modeled as d^{-2} (Kraus 1988), where d is the distance between transmitter (M-pod) and receiver (smartphone). Figure 10 shows the average and standard deviation of RSSI measurements obtained at different distances in real-world experiments. The illustrated noise can result in large errors even for 2-meter zones. Since this noise can be reasonably well modeled as additive white Gaussian noise, in MAQS, multiple readings are used to detect outliers and average values are used to improve distance estimates. Figure 11 shows that the accuracy of proximity detection can be significantly improved when 10 readings are averaged.

Figure 12 illustrates the concept of zone-based information sharing. Numbers along the lines indicate the RSSI between phone and M-pod. In this scenario, phones A and B belong to the zone occupied by M-pod S1, because they are within the required range of S1. Since the RSSI between phone

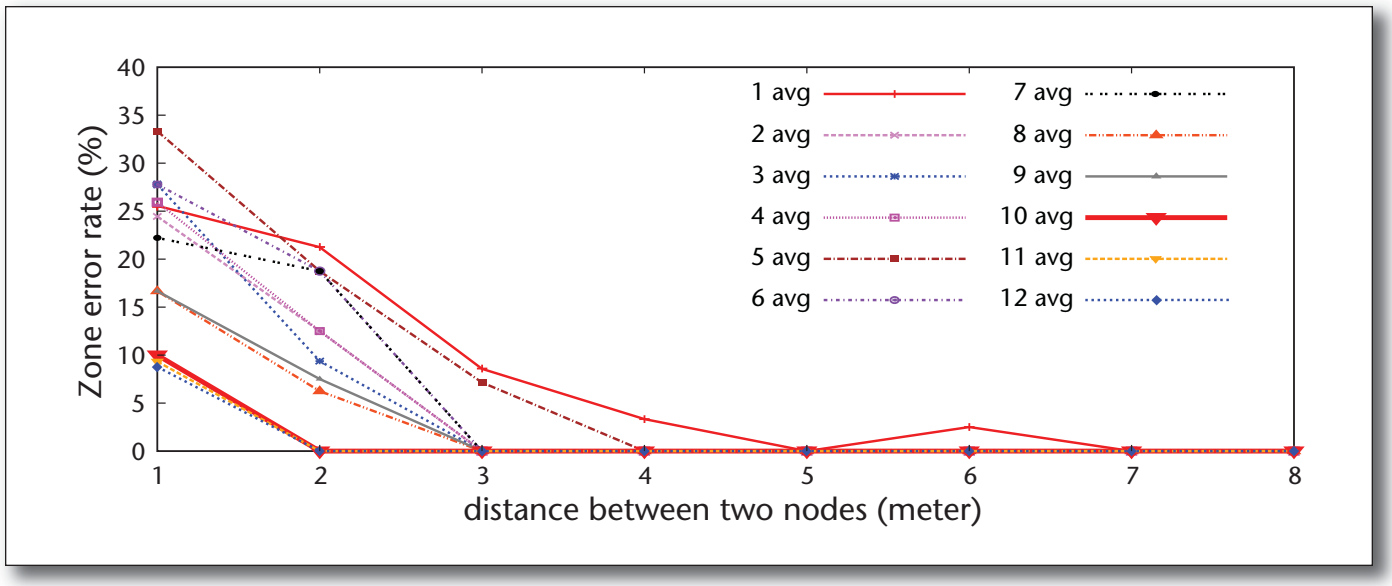

Figure 11. Zone Detection Error Rate Decreases by Averaging Multiple RSSI Readings.

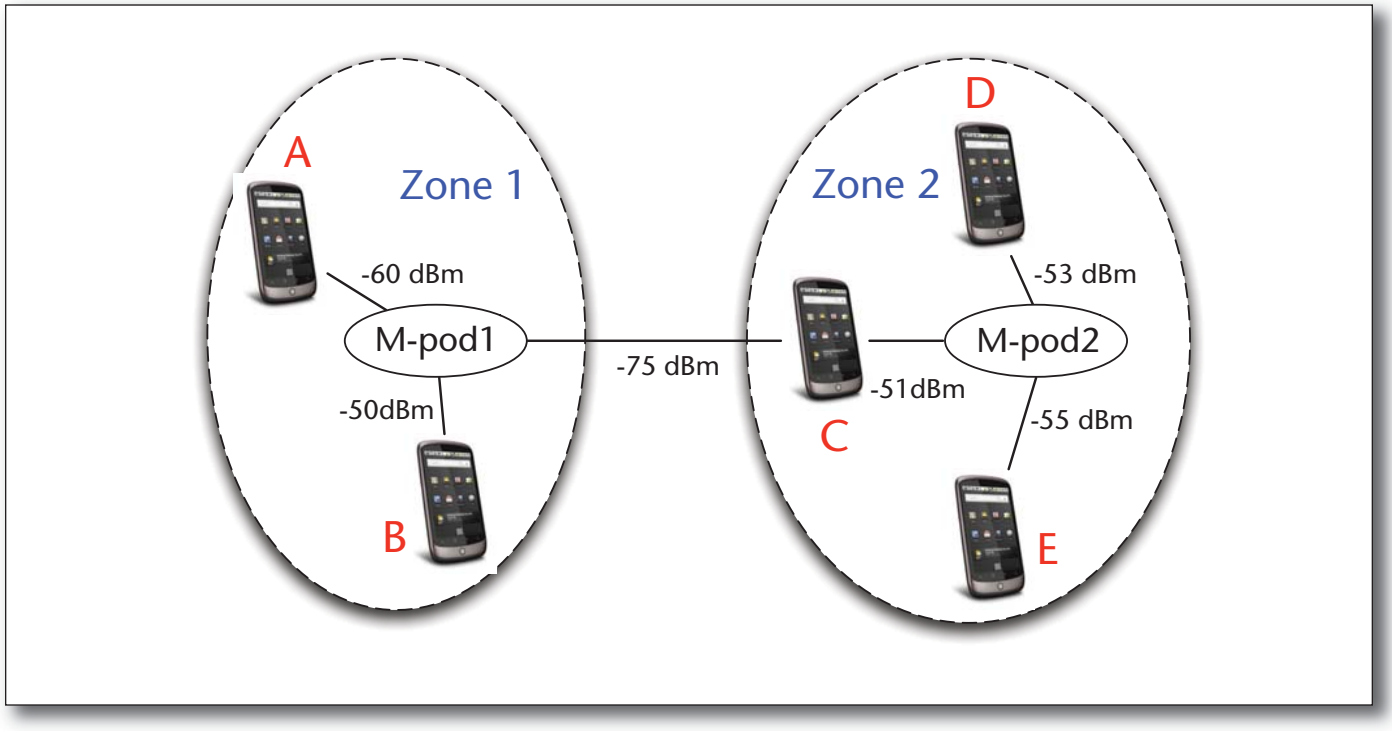

Figure 12. Zone-Based Collaborative Sensing.

C and M-pod S1 is lower than the threshold, they belong to different zones. Note that if two M-Pods are in the same zone but do not have similar pollutant concentration readings, then we will not shut one down as we will need the paired measurements to assess sensor performance and remedy the discrepancy. Further data quality assessment and improvement will be conducted on our server based on those redundant data. If one M-pod consistently reports values that are significantly different from the majority of the other M-pods in the zone, it will be tagged as an outlier, reported to the owner, and will stop sharing its data. If data sharing from an M-pod is occluded in some way, all phones connected to that M-pod will disconnect and the running service will automatically notify the corresponding users and start looking for a new zone to join.

Evaluations

In this section, we describe the system deployment and user study used to evaluate the effectiveness and efficiency of the proposed system. We also make observations based on the data gathered during the user study.

System Deployment and User Study

The deployed MAQS system includes M-pods, smartphones, as well as the data and web servers. We have conducted a two-phase user study with 17 participants, including faculty and graduate students, who share some workplaces and classrooms. The first phase was designed to evaluate our room localization method. In this phase, users were asked to carry their phones for 12 weeks. Our MAQS phone application continuously collected Wi-Fi signals and requested manual labeling when users entered rooms. Weekly meetings with the users were held to verify the accuracy of the motion traces. In the second phase, users carried both smartphones and the M-pod for 3 weeks. The MAQS system collects both room information and IAQ data for all users. This phase of user study allows us to evaluate the entire system. We collected localization data for 171 rooms, and IAQ data for 56 rooms.

Evaluation of Room Localization Technique

We compare our *n*-gram augmented Bayesian room localization model with four state-of-the-art algorithms: (1) Bayesian room localization (Haeberlen et al. 2004; Park et al. 2010), (2) Delta signal Bayesian room localization, which is similar to Bayesian room localization but uses the difference in signal strength (instead of RSS values directly) between each pair of APs to calculate probability, (3) vector-based room localization (Bahl and Padmanabhan 2000), which uses AP RSS vector as the room signature and Euclidean distance to locate the nearest room, and (4) Delta signal vector-based room localization, which is similar to vector-based room localization but uses the difference in signal strength between each pair of APs to build the vectors. As shown in figure 13a, our *n*-gram augmented Bayesian model achieves the best accuracy, especially when the number of fingerprints per room is above 50.

By incorporating the temporal user mobility information, our temporal *n*-gram augmented Bayesian model can achieve better accuracy even when the number of fingerprints per room is limited. As shown in figure 13b, our temporal *n*-gram model further improves the room localization accuracy over our *n*-gram model, especially when the number of fingerprints per room is less than 50. The Delta Bayesian room localization model, which performed second best in figure 13a, can also benefit from the use of temporal user mobility information, but it is still not comparable to our temporal *n*-gram model.

Evaluation of Air-Exchange-Rate-Based IAQ Sensing

To estimate IAQ without using sensors for each specific air pollutant, we propose to calculate the air exchange rate from a time series of CO_2 concentration readings and use this air exchange rate to estimate IAQ. Here, we evaluate the accuracy of the air exchange rate model. We used the Alnor EBT721 Air Balancing Balometer Flow Capture Hood[6] to measure the air-flow rate directly from vents as the ground truth. During each experiment, we change the forced ventilation rate and the number of people in the room to evaluate the accuracy and responsiveness of our CO_2-based air exchange rate model.

Figure 14 shows the results of one experiment. We started at 11:15 A.M. with a relatively high forced ventilation rate and lowered the ventilation rate at 11:30 A.M. We observed that the air exchange rate calculated by our model followed the actual rate drop quickly and stayed within the same range. Starting at 12:15 P.M., we kept the ventilation rate low and changed the number of people in the room every 5 minutes. Again, we can see that the air exchange rate calculated by the model well approximates the measured value. It is slightly higher than the measured value, since the door was opened and closed when we changed the number of people in the room, leading to additional air exchange that is not captured by the vent hood. We conducted multiple experiments in rooms with different sizes and vents, and obtained similar results. Figure 15 shows the accuracy of the air exchange rate sensed by our system, where the *x*-axis shows the time points when Alnor EBT721 was used to collect the ground truth for air exchange rate. The figure demonstrates that our system can measure the air exchange rate with an average accuracy of 90 percent even under a dynamic environment, for example, changes in ventilation and the number of occupants.

Evaluation of Zone-Based Collaborative Sensing

Zone-based collaborative sensing helps to reduce the number of M-pods needed, saves energy, and allow users to share IAQ data. Since the energy consumption of scanning Bluetooth RSSI for a short period of time (less than 30 seconds) is negligible compared with that of continuous IAQ sensing, a zone with *k* devices can generally achieve *k* times better energy efficiency since only one device needs to be running. Here, we evaluate the accuracy of our zone-based proximity detection technique, that is, whether we can identify the cor-

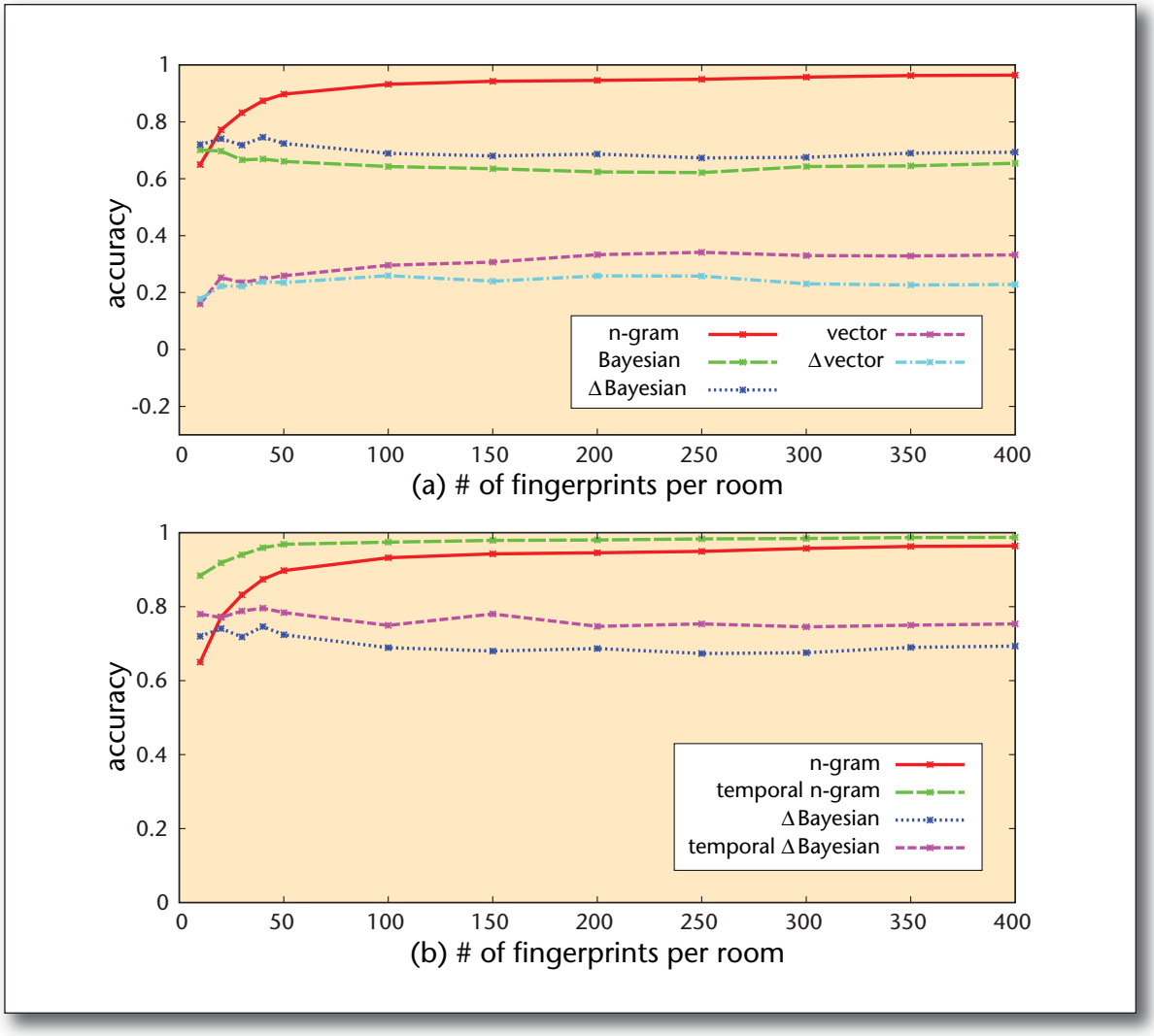

Figure 13. Performance Comparison of Room Localization Methods.

(a) *n*-gram model and (b) temporal *n*-gram model.

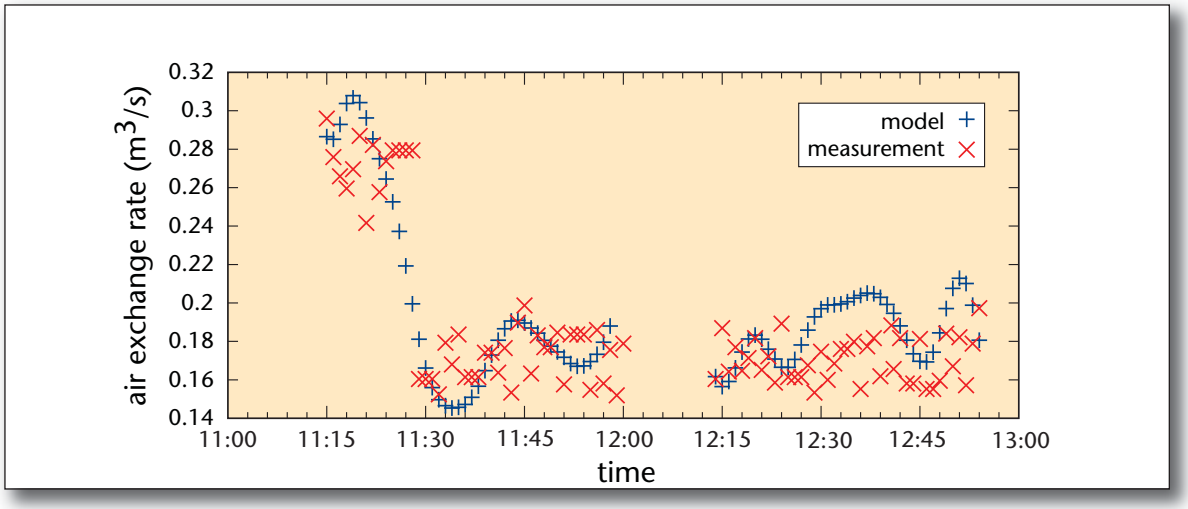

Figure 14. Air Exchange Rate Model Evaluation.

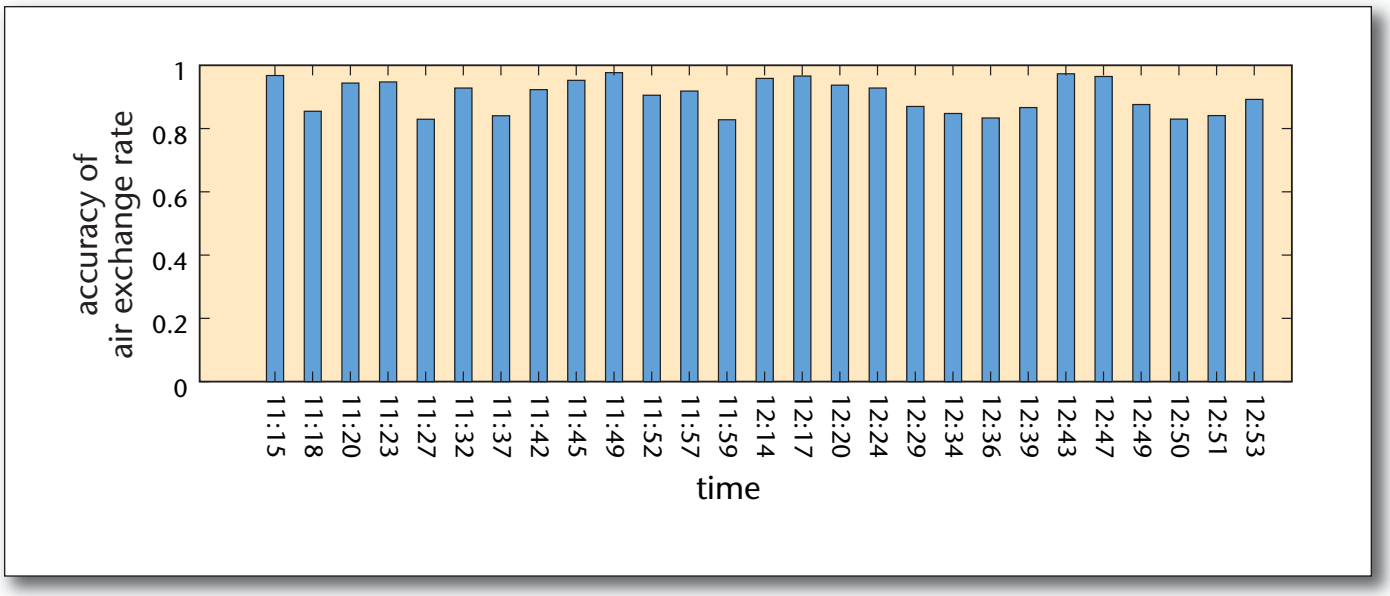

Figure 15. Accuracy of Air Exchange Rate over Time.

rect zone based on the Bluetooth RSSI readings. Given three M-pods and a mobile phone, we selected 10 seat maps that represent real-world user-sitting scenarios. For each seat map, we conducted 10 experiments at different times to capture potential temporal variations. For each experiment, the mobile phone used 10 RSSI readings from each M-pod to determine which zone (that is, M-pod) it belonged to. The average zone detection accuracy for each seat map is shown in table 4. We can see that our RSSI-based zone detection method achieved high accuracy for most seat maps with an average of 89 percent.

Seat Map	1	2	3	4	5
Accuracy (percent)	97	100	100	78	100
Seat Map	6	7	8	9	10
Accuracy (percent)	100	88	100	42	85

Table 4. Zone Detection Accuracy

IAQ Data Analysis

We analyzed the IAQ distributions for the data gathered during our user study. Specifically, we would like to answer quantitatively what IAQ distributions the study participants experienced. Figure 16 shows the IAQ distributions for all users. The dashed lines indicate the standard limits, dark solid lines represent good IAQ, and light solid lines represent bad IAQ. According to the figure, (1) 67 percent of the time, indoor CO_2 concentration is higher than the reasonable limit of 1000 parts per million; (2) 30 percent of the time, air changes per hour do not meet the minimum requirement of 0.35 1/h; and (3) 58 percent of the time, flow rate per person does not meet the minimum standard of 7 l/s/person. We conclude that our study participants frequently spent time in environments with poor air quality.

Figure 17 shows the distributions of CO_2 concentration, air changes per hour, and air flow per person for different users. The users are ordered by their average CO_2 concentrations. We can observe that users are subject to different IAQ at different times, and almost all users are subject to poor IAQ a high percentage of the time (high CO_2, low air changes per hour, or low air flow per person).

Figure 18 shows the distributions of CO_2 concentration, air changes per hour, and air flow per person in different rooms. The rooms are ordered by their average CO_2 concentrations. We can see that rooms have dynamic and diverse IAQ profiles. The IAQ diversity in same room is caused by variation in the number and activities of occupants as well as the ventilation settings. Although the exact fraction is different, many rooms have poor IAQ some of the time.

Related Work

We survey research most relevant to our work on user-centered IAQ monitoring on mobile devices.

IAQ Monitoring

Previous studies (Godwin and Batterman 2007) have focused on monitoring or identifying air pollutants in different types of rooms, such as class-

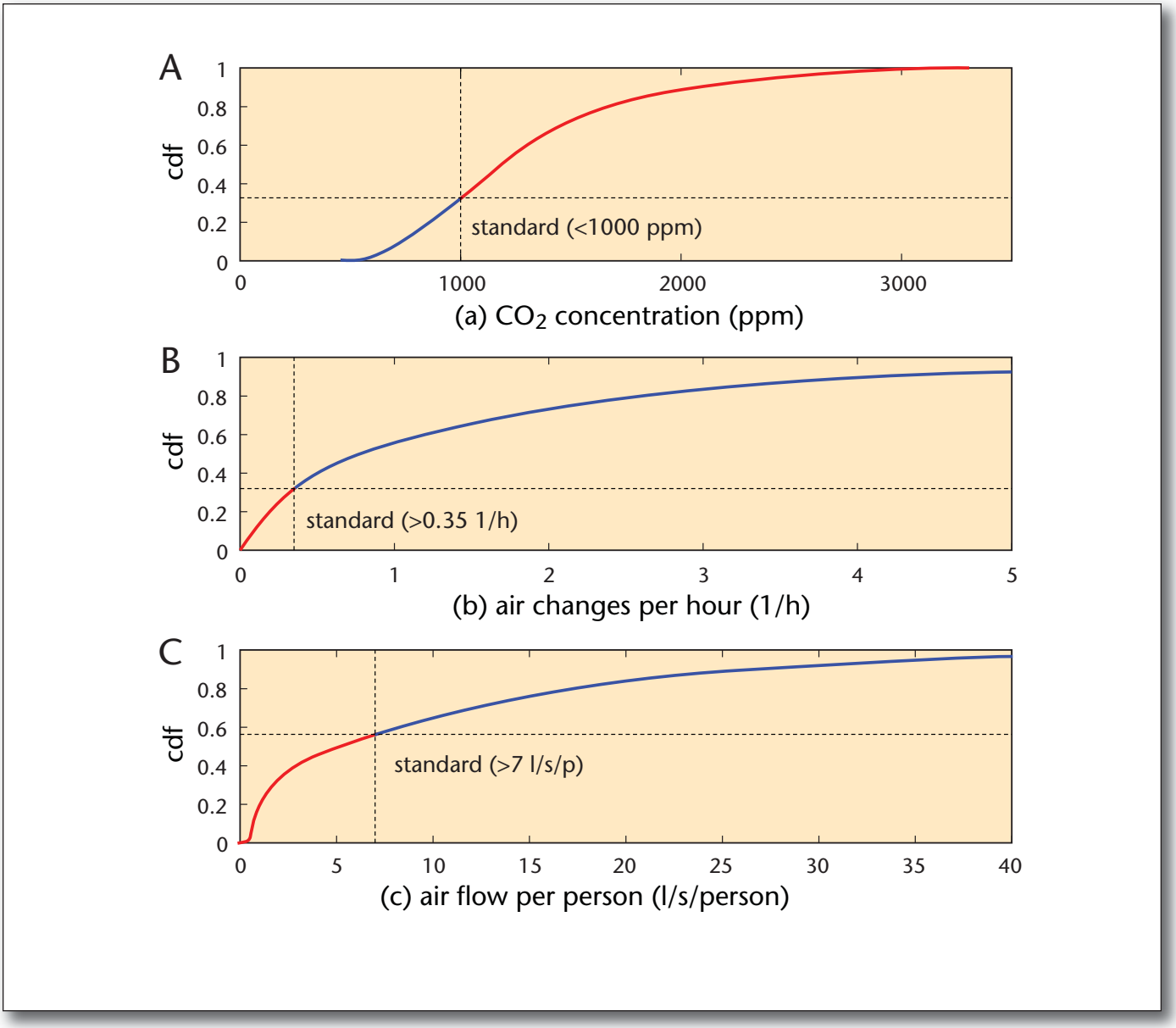

Figure 16. IAQ Data Distribution for All Users.

(a) CO_2 concentration; (b) air changes per hour; and (c) flow rate per person.

rooms, offices, and residential rooms. Other studies have focused on estimating indoor air pollutants in certain areas (for example, city or countryside) using statistical methods. Kim and Paulos (2010)proposed a mobile system for sharing IAQ measurements and visualizations within one's social network. However, the shared information is room based and not user specific.

Indoor Localization

This has been a topic of active research projects, some focusing on indoor intraroom positioning and others (such as ours) focusing on interroom positioning. A number of proprietary systems have been developed, using radio frequency, ultrasound, ZigBee, and so on (Want et al. 1992; Krumm, Cermak, and Horvitz 2003; Sugano 2006). They have good accuracy but require substantial investment in infrastructure and special hardware worn by all users. Other techniques leverage existing wireless infrastructure (Bahl and Padmanabhan 2000), and constructing Wi-Fi fingerprints from Wi-Fi signals to match new/unknown Wi-Fi fingerprints and reference fingerprints at known positions based on proximity or similarity. Constructing the fingerprint database can be labor intensive (Chai and Yang 2007). Therefore, user collaboration based techniques have been proposed (Park et al. 2010).

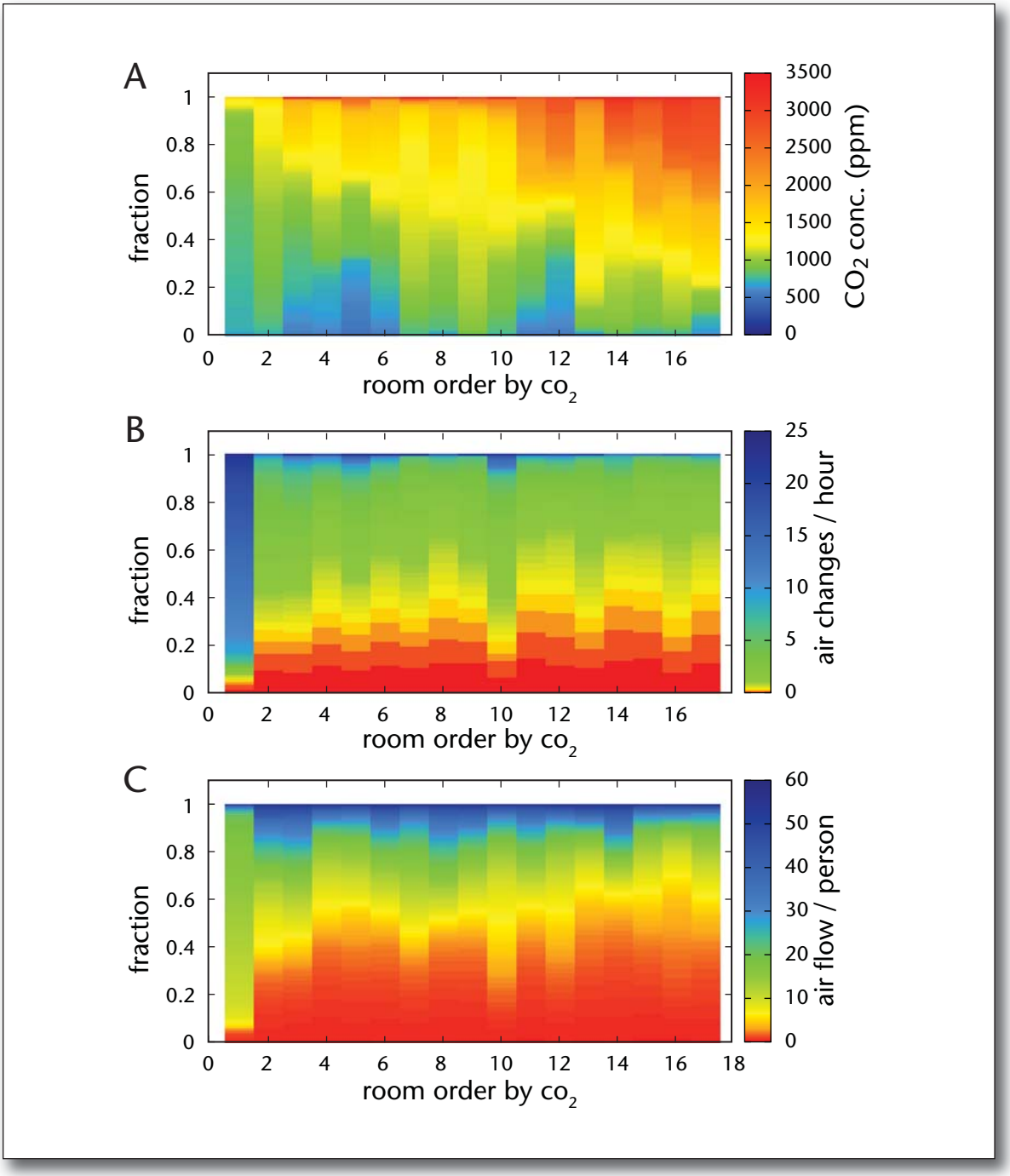

Figure 17. User-Specific Distributions of CO_2 Concentration, Air Changes per Hour, and Air Flow per Person.

However, none of these methods address the challenges associated with environment heterogeneity, device-induced noise, and the requirement for numerous user inputs. Zheng et al. (2008a; 2008b) proposed transferring localization models over time and across multiple devices in order to eliminate environment and device noise in continuous location tracking.

Proximity Detection

Previous peer-based indoor positioning systems attempt to infer either the proximity of a pair of devices, or the actual distances between multiple pairs of devices in order to place them on a virtual map. Most of the techniques use anchors with available position information as references. Other nodes refer to the anchors to determine their

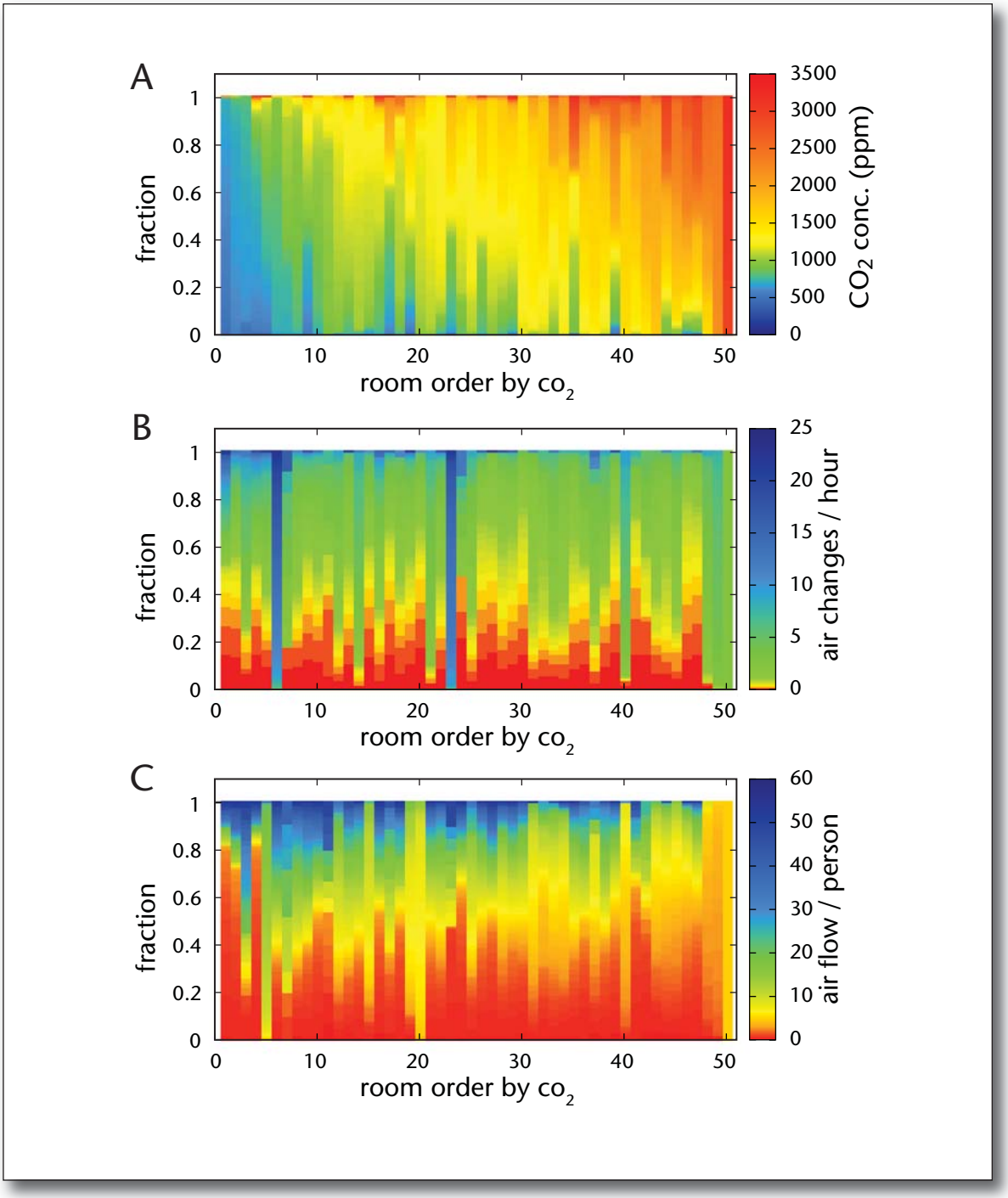

Figure 18. Room-Specific Distributions of CO_2 Concentration, Air Changes per Hour, and Air Flow per Person.

own positions. Examples include PeopleTones (Li et al. 2008), NearMe (Krumm and Hinckley 2004), and Virtual Compass (Banerjee et al. 2010). In our system, precise absolute position is not required; relative proximity information is sufficient. It is conceptually similar to the reality mining system proposed by Nathan Eagle and Alex (Sandy) Pentland (2006). However, mobile devices within a room are distributed more densely and the amount of noise is greater.

Conclusions

This article has described MAQS, a mobile system for personalized IAQ monitoring. To achieve high accuracy and energy efficiency under diverse sens-

ing scenarios, we developed a number of novel techniques: (1) a temporal *n*-gram augmented Bayesian room localization method that achieves high accuracy with a small number of Wi-Fi fingerprints; (2) an air-exchange-rate-based IAQ sensing method that measures general IAQ using only CO_2 sensors; and (3) a zone-based proximity detection method for collaborative sensing, which saves energy and enables data sharing among multiple users. MAQS has been deployed and evaluated through user study. Detailed evaluation results demonstrate the feasibility, effectiveness, and efficiency of MAQS for personalized IAQ monitoring.

Acknowledgements

This material is based upon work supported by the National Science Foundation under awards CNS-0910995, CNS-0910816, and CNS-0347941. We thank Simon Olivieri for his work on the M-pod and Lan Bai for her help with the experiments.

Notes

1. MAQS stands for Mobile Air Quality Sensing.

2. Note that the M-pod integrates multiple air-pollutant sensors and is capable of measuring CO_2, CO, VOCs, ozone, and NO_2. However, it is a flexible monitoring platform and allows users to enable only a subset of the sensors.

3. Arduino BT is available at www.arduino.cc/en/Main/ArduinoBoardBluetooth.

4. www.cdc.gov/niosh/topics/indoorenv/BuildingVentilation.html.

5. See Trends in Atmospheric Carbon Dioxide (www.esrl.noaa.gov/gmd/ccgg/trends/global.html

6. www.aikencolon.com/Alnor-EBT721-EBT-721-Air-Balancing-Balometer-Flow-Capture-Hood_p_2549.html.

References

Bahl, P., and Padmanabhan, V. N. 2000. Radar: An In-Building RF-Based User Location and Tracking System. In *Proceedings of the Nineteenth Annual Joint Conference of the IEEE Computer and Communications Societies*. Los Alamito, CA: IEEE Computer Society.

Banerjee, N.; Agarwal, S.; Bahl, P.; Chandra, R.; Wolman, A.; and Corner, M. 2010. Virtual Compass: Relative Positioning to Sense Mobile Social Interactions. In *Proceedings of the 8th International Conference On Pervasive Computing,* Lecture Notes in Computer Science 6030, 1–21. Berlin: Springer.

Chai, X., and Yang, Q. 2007. Reducing the Calibration Effort for Probabilistic Indoor Location Estimation. *IEEE Transactions on Mobile Computing* 6(6): 649–662.

Daisey, J. M.; Angell, W. J.; and Apte, M. G. 2003. Indoor Air Quality, Ventilation and Health Symptoms in Schools: An Analysis of Existing Information. *Indoor Air* 13(1): 53–64.

Eagle, N., and Pentland, A. (Sandy). 2006. Reality Mining: Sensing Complex Social Systems. *Journal of Personal and Ubiquitous Computing* 10(4): 255–268.

Fisk, W. J.; Mirer, A. G.; and Mendell, M. J. 2009. Quantitative Relationship of Sick Building Syndrome Symptoms with Ventilation Rates. *Indoor Air* 19(2):159–165.

Godwin, C., and Batterman, S. 2007. Indoor Air Quality in Michigan Schools. *Indoor Air* 17(2): 109–121.

Haeberlen, A.; Flannery, E.; Ladd, A. M.; Rudys, A.; Wallach, D. S.; and Kavraki, L. E. 2004. Practical Robust Localization over Large-Scale 802.11 Wireless Networks. In *Proceedings of the 10th Annual International Conference on Mobile Computing and Networking*, 70–84. New York: Association for Computing Machinery.

Huizenga, C.; Abbaszadeh, S.; Zagreus, L.; and Arens, E. 2006. Air Quality and Thermal Comfort in Office Buildings: Results of a Large Indoor Environmental Quality Survey. In *Proceedings of Healthy Buildings*, Vol. III, 393–397. Berkeley, CA: Center for the Built Environment, Center for Environmental Design Research, University of California, Berkeley.

Kim, S., and Paulos, E. 2010. InAir: Sharing Indoor Air Quality Measurements and Visualizations. In *Proceedings of the SIGCHI Conference on Human Factors in Computing Systems*. New York: Association for Computing Machinery.

Kraus, J. D. 1988. *Antennas*. New York: McGraw-Hill.

Krumm, J., and Hinckley, K. 2004. The Nearme Wireless Proximity Server. In *Proceedings of the International Conference on Ubiquitous Computing,* Lecture Notes in Computer Science Volume 3205. Berlin: Springer.

Krumm, J.; Cermak, G.; and Horvitz, E. 2003. Rightspot: A Novel Sense of Location for a Smart Personal Object. In *Proceedings of the International Conference on Ubiquitous Computing,* Lecture Notes in Computer Science Volume 32864. Berlin: Springer.

Li, K. A.; Sohn, T. Y.; Huang, S.; and Griswold, W. G. 2008. Peopletones: A System for the Detection and Notification of Buddy Proximity on Mobile Phones. In *Proceedings of the 6th International Conference on Mobile Systems, Applications, and Services*. New York: Association for Computing Machinery.

Park, J.-G.; Charrow, B.; Curtis, D.; Battat, J.; Minkov, E.; Hicks, J.; Teller, S.; and Ledlie, J. 2010. Growing an Organic Indoor Location System. In *Proceedings of the 8th International Conference on Mobile Systems, Applications, and Services*. New York: Association for Computing Machinery.

Persily, A. 1997. Evaluating Building IAQ and Ventilation with Indoor Carbon Dioxide. *Ashrae Transactions* 103(2)

Seppänen, O. A.; Fisk, W. J.; and Mendell, M. J. 1999. Association of Ventilation Rates and CO_2 Concentrations with Health and Other Responses in Commercial and Institutional Buildings. *Indoor Air* 9(4): 226–252.

Sherman, M. H. 2004. Ashraes First Residential Ventilation Standard. LBNL-54331. Washington, D.C.: U.S. Department of Energy, Lawrence Berkeley National Laboratory Environmental Energy Technologies Division.

Sugano, M. 2006. Indoor Localization System Using RSSI Measurement of Wireless Sensor Network Based on Zigbee Standard. In *Proceedings of the 6th IASTED International Multi-Conference on Wireless and Optical Communications, Wireless Sensor Networks*. Calgary, AB: International Association of Science and Technology for Development.

U.S. Environmental Protection Agency Green Building Workgroup. 2009. *Buildings and their Impact on the Environment: A Statistical Summary*. Washington, DC: U.S. Environmental Protection Agency.

Want, R.; Hopper, A.; Falcaõ, V.; and Gibbons, J. 1992. The Active Badge Location System. *ACM Transactions on Information. Systems* 10(1): 91–102.

Wyon, D. P. 2004. The Effects of Indoor Air Quality on Performance and Productivity. *Indoor Air* 14 Supplement 7: 92–101.

Xiang, Y.; Bai, L. S.; Piedrahita, R.; Dick, R. P.; Lv, Q.; Hannigan, M. P.; and Shang, L. 2012. Collaborative Calibration and Sensor Placement for Mobile Sensor Networks. In *Proceedings of the 11th International Conference on Information Processing in Sensor Networks*. New York: Association for Computing Machinery.

Zheng, V. W.; Pan, S. J.; Yang, Q.; and Pan, J. J. 2008a. Transferring Multi-Device Localization Models Using Latent Multi-Task Learning. In *Proceedings of the 23rd National Conference on Artificial Intelligence*. Menlo Park, CA: AAAI Press.

Zheng, V. W.; Xiang, E. W.; Yang, Q.; and Shen, D. 2008b. Transferring Localization Models over Time. In *Proceedings of the 23rd National Conference on Artificial Intelligence*. Menlo Park, CA: AAAI Press.

Yifei Jiang is a Ph.D. candidate in the Department of Computer Science at the University of Colorado Boulder. He received his M.S. degree from University of Colorado Boulder in 2009 and his B.S. degree from Beijing University of Technology. His research interests span intelligent mobile systems, mobile context sensing, and social networks.

Kun Li received a B.E. degree from Xidian University, Xi'an, China, in 2006. He is currently working toward the Ph.D. degree in the Department of Electrical and Computer and Energy Engineering, University of Colorado Boulder. His work was nominated for the Best Paper Award at ISLPED 2010. His research interests include mobile computing, sensing systems, and cyber physical systems.

Ricardo Piedrahita is a professional research assistant in the Department of Mechanical Engineering at the University of Colorado at Boulder. He received a B.S. in mechanical engineering at the University of California at San Diego in 2007, and an M.S. in mechanical engineering at the University of Colorado at Boulder in 2010. His Master's thesis involved analysis of speciated organics in fine particulate matter and analysis of high frequency coarse particulate matter data from the Denver region. His recent work has been in the field of low-cost air quality sensing techology.

Yun Xiang received his B.S. degree from Zhejiang University and his M.Sc. degree from University of Massachusetts Amherst. He is currently a Ph.D. student at the Department of Electrical Engineering and Computer Science, University of Michigan. Xiang has published in the areas of integrated circuit reliability, online scheduling algorithms, sensor modeling and calibration, and sensor network design and optimization.

Lei Tian is an Ph.D. candidate of the Department of Computer Science, University of Colorado at Boulder. He received his B.S. degree from University of Science and Technology of China in 2010.

Omkar M. Mansata is a system validation engineer at Intel, Austin, Texas. He received his M.S. degree in computer science and engineering (hardware) at the University of Michigan, Ann Arbor in 2011. His research interests include embedded systems, control systems, computer architecture, and VLSI.

Qin Lv is an assistant professor of computer science at the University of Colorado Boulder. She received her B.E. degree with honors from the Department of Computer Science and Technology, Tsinghua University in 2000, her M.A. and Ph.D. degrees from the Department of Computer Science, Princeton University in 2002 and 2006. Before joining University of Colorado, she also spent one year in Princeton University as a postdoc, and one year in the Computer Science Department, Stony Brook University as an assistant professor. Lv's research integrates efficient system design with effective data analysis for the management and exploration of massive data. Her work has won the Computational Sustainability Award by the Computing Community Consortium (CCC) and Pervasive 2012, and the Best Paper Award nomination at ISLPED 2010. Lv has served on the technical program committees of SIGMETRICS, UbiComp, PerCom, and others. Lv's work has been cited more than 2000 times.

Robert P. Dick is an associate professor of electrical engineering and computer science at the University of Michigan. He received his Ph.D. degree from Princeton University in 2002 and his B.S. degree from Clarkson University in 1996. He worked as a visiting professor at the Tsinghua University Department of Electronic Engineering in 2002, as a visiting researcher at NEC Labs America in 1999, and was on the faculty of Northwestern University from 2003–2008. Dick received an NSF CAREER award and won his department's Best Teacher of the Year award in 2004. His technology won a Computerworld Horizon Award and his paper was selected as one of the 30 most influential during the past 10 years in 2007. He is an associate editor of *IEEE Transactions on VLSI Systems*, a guest editor for *ACM Transactions on Embedded Computing Systems*, and serves on the technical program committees of several embedded systems and CAD/VLSI conferences.

Michael Hannigan is an assistant professor in the Department of Mechanical Engineering at the University of Colorado at Boulder. He received his Ph.D. degree in environmental engineering science from Caltech in 1998 and B.S. degree from Southern Methodist University in 1990. He previously held research positions at MIT, Colorado State University, and Denver University. He won his department's Outstanding Undergraduate Teaching Award twice (2007 and 2011), Outstanding Service Award (2008), and Outstanding Research Award (2009).

Li Shang is an assistant professor in the Department of Electrical, Computer, and Energy Engineering, University of Colorado at Boulder. He received his Ph.D. degree from Princeton University in 2004 and his B.S. degree with honors from Tsinghua University. His work was nominated for the Best Paper Award at ISLPED 2010, ICCAD 2008, DAC 2007, and ASP-DAC 2006. His work was selected for publication in *IEEE Micro*'s Top Picks 2006 and won the Best Paper Award at PDCS 2002. He serves as an associate editor of *IEEE Transactions on VLSI Systems* and serves on the technical program committees of several embedded systems, CAD/VLSI, and computer architecture conferences. He won his department's Best Teaching Award in 2006. He received an NSF CAREER award in 2010.